

# Dilution of Dark Matter Relic abundance due to First Order Electroweak Phase Transition in the singlet scalar extended type-II seesaw model

---

**Subhojit Roy**<sup>a,b</sup>

<sup>a</sup>*Harish-Chandra Research Institute, A CI of Homi Bhabha National Institute, Chhatnag Road, Jhansi, Prayagraj (Allahabad) 211019, India*

<sup>b</sup>*Regional Centre for Accelerator-based Particle Physics, Harish-Chandra Research Institute, Prayagraj (Allahabad) 211019, India*

*E-mail:* [subhojitroy@hri.res.in](mailto:subhojitroy@hri.res.in)

**ABSTRACT:** We investigate the effect of a first-order electroweak phase transition (FOEWPT), which is one of the prerequisites for electroweak baryogenesis, on the thermal relic abundance of the dark matter (DM) that freezes out before the phase transition occurs in the complex singlet scalar extended  $Z_3$ -invariant type-II seesaw model that can simultaneously provide a DM candidate, explain the non-vanishing neutrino masses and the baryon asymmetry of the Universe. Such a phase transition around the electroweak scale leaves an impact on the relic density due to the release of entropy, particularly for a TeV-scale DM. We thus concentrate on the region of parameter space of the said model which favors an FOEWPT in the early Universe and for which the DM is heavy such that its freeze-out temperature turns out to be larger than the phase transition temperature. We further study the dependencies of the dilution factor of the DM relic density on the model parameters, the nucleation temperature, the strength and the duration of the phase transition. Such a dilution might retrieve some of the regions of parameter space that were previously ruled out by the measured value of the DM relic density and/or the latest constraints from the DM direct-detection experiments. Furthermore, a direct connection is drawn between the dilution factor and the generation of stochastic gravitational waves as a result of an FOEWPT.

**KEYWORDS:** Beyond Standard Model, Electroweak Phase transition, Dark Matter, Gravitational waves

---

## Contents

<b>1</b>	<b>Introduction</b>	<b>1</b>
<b>2</b>	<b>Dilution of DM relic density due to FOPT</b>	<b>3</b>
<b>3</b>	<b>The theoretical scenario</b>	<b>6</b>
<b>4</b>	<b>Result</b>	<b>10</b>
4.1	TeV-scale scalar DM and the freeze-out temperature	10
4.2	Estimation of the dilution factor	12
4.3	Connection between the produced GW and the Dilution factor	14
<b>5</b>	<b>Conclusions</b>	<b>15</b>
<b>A</b>	<b>Contribution of sound waves to gravitational waves power spectrum</b>	<b>17</b>

---

## 1 Introduction

The relic density of dark matter (DM) in the present Universe is precisely measured from various astrophysical and cosmological experiments, i.e.,  $\Omega_{\text{DM}}h^2 = 0.120 \pm 0.001$  [1]. The particle responsible for the observed DM in the Universe is likely the most wanted new particle after the latest finding of the Standard Model (SM)-like Higgs boson mass around 125 GeV. Among the various possibilities of the nature of the DM, the weakly interacting massive particle (WIMP) still remains a rather viable and the well-motivated DM candidate despite null results from numerous DM experiments and various searches at the Large Hadron Collider (LHC).

The discovery of the Higgs boson [2, 3] at the LHC completes the findings of all the particles appearing in the SM particle physics which vindicates the scheme of spontaneous electroweak symmetry breaking (SSB) as incorporated in the SM. Nevertheless, the electroweak symmetry is restored in the early Universe, i.e., at high temperatures [4]. It is generally understood that SSB transition occurs in the SM via a smooth cross-over [5]. However, in the presence of additional scalars in a scenario beyond the SM (BSM), a first-order phase transition (FOPT) could occur. FOPT at the electroweak scale has an advantage in that it can provide one of the required conditions to explain the baryon asymmetry of the Universe (BAU). The conventional measure of BAU,  $Y_B$ , is the ratio of the difference in the number density of baryon and anti-baryon ( $n_B$  and  $n_{\bar{B}}$ , respectively) and the entropy density ( $s$ ), i.e.,  $Y_B = (n_B - n_{\bar{B}})/s$ . The most accurate value of  $Y_B$  ( $= 8.65 \pm 0.09 \times 10^{-11}$ ) comes from the Planck experiment [6] from its measurement of the baryon acoustic oscillations in the power spectrum of the cosmic microwave background.

In order for baryogenesis to take place, the following three Sakharov requirements [7] must be met: (i) non-conservation of baryon number ( $B$ ), (ii)  $C$  and  $CP$  violations ( $C$ ,  $CP$ ) and (iii) departure from thermal equilibrium. Electroweak baryogenesis (EWBG) is one of the most attractive mechanisms to explain the BAU. It has been widely studied in the literature [8–11] and it requires an FOPT in the electroweak Higgs sector. FOPT fulfils the third criterion of Sakharov’s conditions, i.e., the system has to go out of thermal equilibrium. In addition, the phase transition has to be strongly first-order to avoid a wash-out of the created baryons inside the broken EW phase [12].

The study of FOPT at around the electroweak scale has recently gained heightened attention, particularly after the recent observation of gravitational waves (GW) from LIGO and VIRGO collaboration [13–16]. This is since FOPT would be responsible for possible stochastic GW which might act as a background for the various future space/ground-based GW experiments, viz., LISA [17], ALIA [18], Taiji [19], TianQin [20], aLigo+ [21], Big Bang Observer (BBO) [22] and Ultimate(U)-DECIGO [23]. Note that EWPT in the SM is unable to generate any GW since the transition is of a cross-over type. Therefore, detection of such type of a stochastic GW would likely point to BSM physics.

In addition, an FOPT in the early Universe can significantly impact the thermal history of those particle(s) species that freeze out before the phase transition. During the phase transition of the Universe from a false to the true vacuum, the relic density of those species is diluted due to an injection of entropy and a release of latent heat. Today’s relic abundance of the thermal species that decouple after the phase transition would not be affected as a thermal equilibrium attained after the phase transition would erase the effect of dilution.

The effect of dilution on the DM relic density would be significant when the temperature of the FOPT happens to be smaller than the DM freeze-out temperature. Such an effect would therefore be important in the context of a first-order electroweak phase transition (FOEWPT) for DM candidates with TeV-scale masses ( $m_\chi$ ) which are expected to get frozen out from the thermal equilibrium at a freeze-out temperature ( $T_{FO}$ ) around the electroweak scale ( $T_{FO} \simeq \frac{m_\chi}{25}$ ). The dilution of thermal relic abundance of DM due to FOPT has been studied in the past by considering some toy-model-like effective potential such as adding a larger degree of freedom from the hidden sector [24–27]. Recently, it has been studied in more realistic models such as a singlet extension of the SM (xSM) and two-Higgs-doublet model (2HDM+S) in reference [28].

Apart from the issues pertaining to DM and BAU, another shortcoming of the SM is that it considers the neutrinos to be massless while various experiments have established that neutrinos indeed have mass [29, 30]. In this work, we consider  $Z_3$ -symmetric complex singlet scalar extension type-II seesaw model which has a natural explanation of the origin of finite neutrino mass, provides a singlet scalar DM candidate and can generate the observed baryon asymmetry of the Universe via the EWBG. In contrast to the type-I and type-III seesaw models, type-II seesaw model permits large neutrino Yukawa couplings via a small triplet vacuum expectation value concurrently even with a sub-TeV seesaw. In addition, new interactions between the SM Higgs doublet and the complex triplet could modify the Higgs potential in favour of an FOPT. The interplay among the production of GW, DM and physics

at the LHC has been studied in this model in reference [31]. Recently, it has been shown that this model can explain the observed excess of electron-positron flux from AMS-02 [32], DAMPE [33] and Fermi-LAT [34] collaborations [35]. The present work aims to investigate a possible dilution of the relic abundance of a heavy singlet-like scalar DM due to an FOPT in the Higgs sector around the electroweak scale. We calculate the magnitude of the dilution factor and point out the region of the relevant parameter space where such a dilution could be significant. Furthermore, a direct connection between the dilution factor and the generation of stochastic GW as a result of an FOEWPT is also discussed.

The present work is organized as follows. We briefly review how an FOPT affects the relic abundance of DM particles that freeze out later than the transition temperature in section 2. The detailed description of the model is discussed in section 3. We present our results in section 4. In section 5, we conclude. The estimation of the production of stochastic GW from sound waves is discussed in the appendix A.

## 2 Dilution of DM relic density due to FOPT

In this section, we discuss the dilution of thermal DM due to the release of entropy during an FOPT that occurs at a considerably lower temperature than  $T_{\text{FO}}$ . The dilution factor depends critically on the temperature at which FOPT occurs. Thus, we will start off by talking about the study of phase transition of the effective scalar potential at finite temperature. We will later go over how to estimate the dilution factor due to the release of entropy during the FOPT.

When the finite-temperature effective Higgs potential,  $V(\phi, T)$ , exhibits (at least) two local minima that are already separated by a barrier, an FOEWPT can start to occur in the early Universe. In the hot and radiation-dominated era of the early Universe at high temperatures, the minimum of the scalar potential is at the origin in the field space ( $\phi = 0$ ), i.e., the electroweak symmetry is unbroken. As the temperature drops due to the expansion of the Universe, a second minimum away from the origin in the field value ( $\phi = \phi_{\text{broken}}$ ) may develop at which  $V(\phi_{\text{broken}}, T) > V(0, T)$ . Note that the value of  $\phi_{\text{broken}}$  varies with temperature. With the drop in the temperature of the Universe,  $V(\phi_{\text{broken}}, T)$  starts to decrease relative to  $V(0, T)$  and at some temperature  $T = T_c$ , where  $T_c$  is known as the ‘critical temperature of the phase transition, both the two minima become degenerate. As the temperature continues to drop further below  $T_c$ , the minimum at  $\phi = \phi_{\text{broken}}$  becomes the global minimum of the effective potential while the minimum at the origin is now considered to be a false minimum. When there is a barrier between the two minima, the system can start to tunnel from the false minimum to the true global minimum of the potential. As a result, at a certain temperature  $T < T_c$ , a phase transition like this one, known as a first-order type phase transition, can take place in the early Universe.

The model of bubble nucleation is an effective way to describe this type of tunnelling process. Because of the large surface tension of the bubble walls compared with the energy difference between the two minima, most of the bubbles of the broken minimum remain small and finally collapse. The bubble of the broken phase nucleates in the cosmological plasma,

in which the electroweak symmetry is unbroken, when the rate of nucleation per unit volume ( $\Gamma$ ) is larger than the Hubble expansion rate. A bubble that is already formed in the plasma continues to develop, collide, and coalesce with other bubbles which are also forming until a big bubble is created. In this manner, the whole space is engulfed and EWSB spreads across the entire field-space. At finite temperatures ( $T$ ), in the semi-classical approximation the tunnelling probability from the false vacuum to the true vacuum per unit time per unit volume is given by [36]

$$\Gamma(T) \simeq T^4 \left( \frac{S_3(T)}{2\pi T} \right)^{3/2} e^{-S_3(T)/T}, \quad (2.1)$$

where the three-dimensional Euclidean action  $S_3(T)$  of the background field ( $\phi$ ), in the spherical polar coordinate, is given by

$$S_3(T) = 4\pi \int dr r^2 \left[ \frac{1}{2} \left( \partial_r \vec{\phi} \right)^2 + V \right]. \quad (2.2)$$

By extending this Euclidean action, it is possible to determine the prerequisite of the formation of a bubble of a critical size. In this work, we consider the publicly accessible package **CosmoTransitions** [37] for this investigation and to calculate the bounce solution for the aforementioned Euclidean action. The nucleation temperature can be found by solving the following equation:

$$\int_{T_n}^{\infty} \frac{dT}{T} \frac{\Gamma(T)}{H(T)^4} \simeq 1. \quad (2.3)$$

The above relation indicates that the probability of a single bubble nucleating inside one horizon volume is around 1. It estimates the required condition  $S_3(T)/T \approx 140$  to obtain the nucleation temperature ( $T_n$ ) of the phase transition [38].  $T_n$  is the highest temperature at which  $S_3/T \lesssim 140$ . The absolute values of  $T_c$ ,  $T_n$  and their difference ( $\Delta T_{cn} = T_c - T_n$ ) have a significant impact on the dilution factor of the relic density of DM due to FOPT.

Depending on the value of  $\Delta T_{cn}$ , the study of dilution of DM relic density due to the release of entropy caused by an FOPT can be classified into two cases. First, consider the case where  $\Delta T_{cn}$  is small. Here, the temperature at which the phase transition occurs is close to the critical temperature of the effective potential which corresponds to negligible supercooling [9, 25]. In this scenario, the total entropy is conserved as the system is almost in the equilibrium, i.e.,  $sa^3$  is conserved where ‘ $s$ ’ denotes the entropy density and ‘ $a$ ’ represents the scale factor of the expansion of the Universe. Therefore the entropy density of a phase can be found using this conservation relation. In the following discussion,  $+$  ( $-$ ) indicates the high-temperature symmetric (low-temperature broken) phase and the subscript  $i$  ( $f$ ) denotes the beginning (end) of the FOPT. Due to the release of entropy during an FOPT, the entropy density changes as

$$s_- = \left( \frac{a_i}{a_f} \right)^3 s_+. \quad (2.4)$$

Thus, in this scenario, the dilution factor due to an FOPT is given by

$$d \equiv \left( \frac{a_f}{a_i} \right)^3 = \left( \frac{s_+(T_c)}{s_-(T_n)} \right). \quad (2.5)$$

The second case corresponds to the larger  $\Delta T_{cn}$  scenario, i.e., when  $T_n \ll T_c$ . Equation 2.4 does not hold as the symmetric and the broken phases are no longer in equilibrium at the beginning of the phase transition. The evolution of the phase transition in this category can be described in three distinct stages: supercooling, reheating, and phase coexistence. The high-temperature phase dominates the Universe during the supercooling stage wherein the entropy remains conserved. Therefore, similar to equation 2.4 the following relation can be found

$$\left(\frac{a_i}{a_s}\right)^3 = \left(\frac{s_+(T_n)}{s_+(T_c)}\right), \quad (2.6)$$

where  $a_s$  is the scale factor at the end of the supercooling stage, i.e., near  $T \simeq T_n$ . At the end of the supercooling stage, the release of the latent heat reheats the Universe. The overall energy density of the Universe,  $\rho$ , does not change if the reheating proceeds far faster than the Universe expansion rate. However, in this situation entropy does not continue to be preserved. The Universe can reach the stage of phase coexistence at  $T = T_c$  if a significant amount of reheating takes place. Its energy density would then be given by

$$\rho_-(T_c) = f\rho_-(T_c) + (1-f)\rho_+(T_c), \quad (2.7)$$

where  $f$  is the volume fraction of the plasma of the low-temperature phase at the beginning of the phase coexistence which can be found from the energy conservation relation given by

$$\rho_+(T_n) = \rho_-(T_c). \quad (2.8)$$

Using equations 2.7 and 2.8, we can find the following relation for  $f$ , i.e.,

$$f = \frac{\rho_+(T_c) - \rho_+(T_n)}{L}, \quad (2.9)$$

where  $L (= \rho_+(T_c) - \rho_-(T_c))$  denotes the transition latent heat at  $T = T_c$ . Finally, the process of the third stage, i.e., the phase coexistence stage, occurs very quickly such that the total entropy again remains conserved which leads to the following relation:

$$a_s^3[(1-f)s_+(T_c) + fs_-(T_c)] = a_f^3s_-(T_c). \quad (2.10)$$

The left- and right-hand sides of the above relation correspond to the total entropy at the beginning and at the end of this stage, respectively. It can be expressed as

$$\left(\frac{a_s}{a_f}\right)^3 = \frac{1 - \Delta s/s_+(T_c)}{1 - f\Delta s/s_+(T_c)}, \quad (2.11)$$

where  $\Delta s = s_+(T_c) - s_-(T_c)$ . Therefore, by combining equations 2.6 and 2.11, it is possible to find the dilution factor for this scenario and it is given by

$$d \equiv \left(\frac{a_f}{a_i}\right)^3 = \left(\frac{1 - f\Delta s/s_+(T_c)}{1 - \Delta s/s_+(T_c)}\right) \left(\frac{s_+(T_c)}{s_+(T_n)}\right). \quad (2.12)$$

In this work, we use this relation to estimate the dilution of the DM relic density caused by an FOPT in section 4.

In addition, FOPT in the early Universe could generate stochastic GW. Such a GW signal can be estimated from the four portal parameters that are related to the phase transition in the scalar potential and those are  $T_n, \alpha, \beta/H_n$  and  $v_w$  where ‘ $\alpha$ ’ is a dimensionless quantity which is related to the energy budget of the FOPT,  $\beta/H_n$  estimates the inverse duration of the phase transition and  $v_w$  is the bubble wall velocity. Definitions of these parameters are shown in Appendix A. Such a GW from an FOPT is generally produced via three distinct processes: bubble wall collisions [39, 40], long-standing sound waves in the plasma [41–44] and magnetohydrodynamic (MHD) turbulence [45–50]. Among all these, the sound wave contribution is the dominant contribution to the peak of the GW intensity. Various relations from that computation are presented in Appendix A. We use these relations to study the connection between the dilution of the DM relic density and the produced stochastic GW resulting from an FOPT.

Before ending this section, note that there are some prerequisites in estimating the dilution factor. It is related to the assumption that the released latent heat after the supercooling reheats the Universe which brings the temperature back to a temperature just close to  $T_c$ . Observe that the value of the variable  $f$ , that estimates the plasma volume fraction of the low-temperature phase at the starting of the phase coexistence stage, can not be larger than 1 in equations 2.7 and 2.8. However, in some situations, particularly when the dilution factor is large, the value of  $f$  can exceed the value 1 using the relation in equation 2.9. The underlying assumption made above has the explanation behind this. When  $T_n \ll T_c$ , the large amount of released latent heat cannot bring the system to a temperature close to  $T_c$ . In this scenario, for the correct estimation of the dilution factor,  $T_n$  needs to be replaced by the reheating temperature  $T_r$  in equation 2.12. Although  $T_r$  estimation is beyond the scope of this work as such a calculation consider specific kinetic processes [25]. If we neglect the contributions from the terms that includes  $f$ , i.e., considering  $f = 1$ , in equation 2.12 the relation of dilution factor becomes  $d \equiv \left(\frac{a_f}{a_i}\right)^3 = \left(\frac{s_+(T_c)}{s_+(T_n)}\right) = \left(\frac{T_c}{T_n}\right)^3 = \left(1 + \frac{\Delta T_{\text{cn}}}{T_n}\right)^3$  [28]. This relation actually estimates a much-enhanced dilution factor. In addition, in the realistic scenario, friction will drastically reduce the mobility of bubble walls in the plasma-wall system. The collisions of the walls of the bubbles of the true broken phase also release entropy and enhance the dilution factor [26]. Therefore, refuting the underline assumption does not imply a reduction in the dilution factor that we estimate in this work.

### 3 The theoretical scenario

The current model is an extension of the SM with a  $SU(2)_L$  scalar triplet,  $\Delta$ , with hypercharge,  $Y = 2$ , and a complex scalar singlet,  $S$ , which transforms non-trivially under a  $Z_3$ -discrete symmetry [31, 35]. The discrete  $Z_3$ - symmetry stabilises the singlet field, i.e., it does not develop  $vev$  on EWSB and becomes the DM candidate of the model. In Table 1, we present various quantum numbers of various scalars of the scenario under the extended gauge group  $SU(3)_C \times SU(2)_L \times U(1)_Y \times Z_3$ . The Lagrangian of the model is given by

$$\mathcal{L}_{\text{tot}} = \mathcal{L}_{\text{Kinetic}} + \mathcal{L}_{\text{Yukawa}} - \mathcal{V}(H, \Delta, S). \quad (3.1)$$

Fields		$\underbrace{SU(3)_C \otimes SU(2)_L \otimes U(1)_Y}_{\text{SM}} \otimes Z_3$			
Complex Scalar DM	$s = \frac{1}{\sqrt{2}}(h_s + ia_s)$	1	1	0	$e^{i\frac{2\pi}{3}}$
Scalar Triplet	$\Delta = \begin{pmatrix} \frac{\Delta^+}{\sqrt{2}} & \Delta^{++} \\ \frac{1}{\sqrt{2}}(h_t + ia_t) & -\frac{\Delta^+}{\sqrt{2}} \end{pmatrix}$	1	3	2	1
Higgs doublet	$H = \begin{pmatrix} G^+ \\ \frac{1}{\sqrt{2}}(h_d + ia_d) \end{pmatrix}$	1	2	1	1

**Table 1.** Assignments of charges on the scalar fields under the gauge group  $\mathcal{G} \equiv \mathcal{G}_{\text{SM}} \otimes Z_3$  where  $\mathcal{G}_{\text{SM}} \equiv SU(3)_C \otimes SU(2)_L \otimes U(1)_Y$ . The hypercharges ( $Y$ ) are obtained by using the relation:  $Q = I_3 + \frac{Y}{2}$ , where  $Q$  is the electromagnetic charge and  $I_3$  is the third component of isospin.

where

$$\mathcal{L}_{\text{Kinetic}} = (D^\mu H)^\dagger D_\mu H + (D^\mu \Delta)^\dagger D_\mu \Delta + (\partial^\mu S)^\dagger \partial_\mu S, \quad (3.2)$$

$$\mathcal{L}_{\text{Yukawa}} = \mathcal{L}_{\text{Yukawa}}^{\text{SM}} - (y_L)_{\alpha\beta} \overline{L}_\alpha^c i\sigma^2 \Delta L_\beta + h.c., \quad (3.3)$$

with

$$\begin{aligned} D_\mu H &= \left( \partial_\mu - ig_2 \frac{\sigma^a}{2} W_\mu^a - ig_1 \frac{Y_H}{2} B_\mu \right) H, \\ D_\mu \Delta &= \partial_\mu \Delta - ig_2 \left[ \frac{\sigma^a}{2} W_\mu^a, \Delta \right] - ig_1 \frac{Y_\Delta}{2} B_\mu \Delta. \end{aligned} \quad (3.4)$$

Here,  $y_L$  is a  $3 \times 3$  complex symmetric matrix.  $g_1$  and  $g_2$  are the  $U(1)$  and the  $SU(2)$  gauge couplings, respectively. The heavy triplet scalar helps us to generate neutrino masses through the standard type-II seesaw mechanism. Neutrino masses are generated once the neutral triplet scalar gets non-zero  $vev$  after the EWSB. The representations of the Higgs doublet ( $H$ ), the triplet scalar ( $\Delta$ ) and the singlet scalar ( $S$ ) are shown in table 1. After the EWSB,  $vev$  of the neutral  $CP$ -even field of  $H$  ( $\Delta$ ) is denoted by  $v_d$  ( $v_t$ ) where  $v = \sqrt{v_d^2 + 2v_t^2} = 246$  GeV. The scalar potential of the model is given by:

$$\begin{aligned} V(H, \Delta, S) &= -\mu_H^2 (H^\dagger H) + \lambda_H (H^\dagger H)^2 \\ &+ \mu_\Delta^2 \text{Tr} [\Delta^\dagger \Delta] + \lambda_1 (H^\dagger H) \text{Tr} [\Delta^\dagger \Delta] + \lambda_2 \left( \text{Tr} [\Delta^\dagger \Delta] \right)^2 \\ &+ \lambda_3 \text{Tr} [(\Delta^\dagger \Delta)^2] + \lambda_4 (H^\dagger \Delta \Delta^\dagger H) + \left[ \mu (H^T i\sigma^2 \Delta^\dagger H) + h.c. \right] + \mu_S^2 |S|^2 \\ &+ \lambda_S |S|^4 + \frac{\mu_3}{3!} (S^3 + S^{*3}) + \lambda_{SH} H^\dagger H (S^* S) + \lambda_{S\Delta} \text{Tr} [\Delta^\dagger \Delta] (S^* S). \end{aligned} \quad (3.5)$$

In this work, we consider all the Lagrangian parameters to be real. Thus, there is no spontaneous  $CP$  violation in our scenario. The bare masses ( $\mu_H^2$  and  $\mu_\Delta^2$ ) can be obtained by minimising the scalar potential for the field values at the vacuum. The mass of the singlet scalar DM after the EWSB is given by

$$m_S^2 = \mu_S^2 + \frac{1}{2} \lambda_{SH} v_d^2 + \frac{1}{2} \lambda_{S\Delta} v_t^2. \quad (3.6)$$



On EWSB, the doublet and the triplet scalars would mix. The neutral scalar mass-matrix, on diagonalization, gives rise to two  $CP$ -even scalars  $h^0$  and  $H^0$ . These are given by,

$$h^0 = h_d \cos \theta_t + h_t \sin \theta_t, \quad H^0 = -h_d \sin \theta_t + h_t \cos \theta_t, \quad (3.7)$$

where  $\theta_t$  represents the mixing angle of the diagonalizing matrix and is given by

$$\tan 2\theta_t = \frac{\sqrt{2}\mu v_d - (\lambda_1 + \lambda_4)v_d v_t}{M_\Delta^2 - \frac{1}{4}\lambda_H v_d^2 + (\lambda_2 + \lambda_3)v_t^2}, \quad (3.8)$$

where  $M_\Delta^2 = \frac{\mu v_d^2}{\sqrt{2}v_t}$ . The corresponding mass eigenvalues of these physical eigenstates are given by

$$\begin{aligned} m_{h^0}^2 &= (M_\Delta^2 + 2v_t^2(\lambda_2 + \lambda_3)) \sin^2 \theta_t + 2\lambda_H v_d^2 \cos^2 \theta_t - \frac{v_t \sin 2\theta_t (2M_\Delta^2 - v_d^2(\lambda_1 + \lambda_4))}{v_d}, \\ m_{H^0}^2 &= (M_\Delta^2 + 2v_t^2(\lambda_2 + \lambda_3)) \cos^2 \theta_t + 2\lambda_H v_d^2 \sin^2 \theta_t + \frac{v_t \sin 2\theta_t (2M_\Delta^2 - v_d^2(\lambda_1 + \lambda_4))}{v_d}. \end{aligned} \quad (3.9)$$

For  $m_{h^0} < m_{H^0}$ , the lighter eigenstate  $h^0$  mimics the SM Higgs boson with mass  $m_{h_{\text{SM}}} = 125$  GeV. Similarly, the mixing between two  $CP$ -odd states ( $a_d, a_t$ ) would project out the massless Nambu-Goldstone mode and one massive pseudoscalar,  $A^0$  with its mass given by

$$m_{A^0}^2 = \frac{M_\Delta^2 (4v_t^2 + v_d^2)}{v_d^2}. \quad (3.10)$$

A similar orthogonal rotation in the singly-charged scalar sector comprising of  $G^\pm$  and  $\Delta^\pm$  fields would lead to one massless Nambu-Goldstone state which shows up as the longitudinal components of the massive  $W^\pm$ -bosons and the charged scalar  $H^\pm$ . The mass of  $H^\pm$  is given by

$$m_{H^\pm}^2 = \frac{(2v_t^2 + v_d^2)(4M_\Delta^2 - \lambda_4 v_d^2)}{4v_d^2}. \quad (3.11)$$

The mass of the doubly charged scalar  $H^{\pm\pm} (\equiv \Delta^{\pm\pm})$  is given by

$$m_{H^{\pm\pm}}^2 = M_\Delta^2 - \lambda_3 v_t^2 - \frac{\lambda_4 v_d^2}{2}. \quad (3.12)$$

Note that the constraint on  $m_{H^{\pm\pm}}$  from the various heavy Higgs searches at the LHC mostly depends on  $v_t, m_{H^{\pm\pm}}$  and the mass difference  $\Delta m (= m_{H^{\pm\pm}} - m_{H^\pm})$ . At the limit  $v_t^2/v_d^2 \ll 1$ ,  $\Delta m$  can be found from the following relation:

$$(m_{H^{\pm\pm}}^2 - m_{H^\pm}^2) \approx -\frac{\lambda_4 v_d^2}{4}; \quad (m_{H^\pm}^2 - m_{A^0}^2) \approx -\frac{\lambda_4 v_d^2}{4}; \quad m_H \approx m_A^0 \approx M_\Delta. \quad (3.13)$$

Thus, sign of  $\lambda_4$  generates two types of the mass hierarchy among  $H^{\pm\pm}, H^\pm, H^0/A^0$ . For  $\lambda_4 < 0$  ( $> 0$ ) the mass ordering is  $m_{H^{\pm\pm}} > m_{H^\pm} > m_{H^0, A^0}$  ( $m_{H^{\pm\pm}} < m_{H^\pm} < m_{H^0, A^0}$ ).

Various theoretical constraints such as stability, unitarity, perturbativity and the latest experimental constraints from the dark sector as well as from the various LHC searches, the constraints from the flavor and neutrino sectors and the constraints from the electroweak precision data observables such as  $\rho$ ,  $S$ ,  $T$ ,  $U$  parameters have been discussed in detail in reference [31].

In the present work, we focus on that kind of parameter space region exhibiting an FOEWPT in the early Universe. Such a scenario prefers the triplet sector scalars to be lighter. However, the null results from various collider searches that have been carried out over the years at the LHC [51–60] to hunt those triplet-like scalar excitations, strongly constrain the parameter space of the type-II seesaw sector of the present model. Such a bound on  $m_{H^{\pm\pm}}$  mostly depend on  $\Delta m$ ,  $v_t$  and the value of  $m_{H^{\pm\pm}}$ . In the scenario when  $\Delta m = 0$ , the ATLAS collaboration finds the most stringent bound to be  $m_{H^{\pm\pm}} \gtrsim 870$  GeV. This was accomplished by making the assumption that  $\text{BR}(H^{\pm\pm} \rightarrow \mu^\pm \mu^\pm)$  is 100% [57], which corresponds to a smaller  $v_t$  region, using  $36.1 \text{ fb}^{-1}$  data at  $\sqrt{s} = 13$  TeV. On the other hand, a different ATLAS analysis assuming 100% branching fraction of  $H^{\pm\pm}$  to the  $W^\pm W^\pm$  final state, that corresponds to the larger  $v_t$  region, excludes on  $m_{H^{\pm\pm}} \gtrsim 350$  GeV [60] with  $139 \text{ fb}^{-1}$  data. In the case of  $\Delta m < 0$  the bound is much stronger. In this scenario, the effective production cross-section of  $H^{\pm\pm}$  at the LHC increases as it can produce from the cascade decays of  $H^0/A^0$  and  $H^\pm$ . By recasting several ATLAS and CMS results, it has been shown in a recent study [61] that the existing exclusion limit for  $m_{H^{\pm\pm}}$  is 1115 (1076) GeV for  $\Delta m = -10$  (–30) GeV with  $v_t \sim 10^{-5} - 10^{-6}$  GeV. On the contrary, the bound on  $m_{H^{\pm\pm}}$  relaxes a lot in the case of  $\Delta m > 0$ .

The scenario with  $\Delta m > 0$ , the neutral triplet-like scalar  $H^0$  and  $A^0$  mostly decay to invisible neutrinos for  $v_t < 10^{-4}$  GeV [61]. Thus the produced  $H^{\pm\pm} H^{\mp\mp}$  and  $H^{++} H^{--}$  yields soft-leptons/jets in the final states. Since the particles are very soft, it is difficult to reconstruct them at the LHC. Recently, by recasting various ATLAS and CMS analyses in reference [61], it has been shown that LHC would be unable to constrain the parameter space of  $\Delta m = 10$  GeV (30 GeV),  $v_t$  around  $10^{-3}$  GeV to  $10^{-5}$  GeV ( $10^{-3}$  GeV to  $10^{-6}$  GeV) and  $m_{H^{\pm\pm}} \gtrsim 200$  GeV at  $3 \text{ ab}^{-1}$  integrated luminosity data.

Therefore, the region of parameter space of the triplet sector that we consider for this work corresponds to,<sup>1</sup>

$$\{10 \text{ GeV} < \Delta m < 40 \text{ GeV}\} \Rightarrow \lambda_4 < 0 ; \{10^{-6} \text{ GeV} < v_t < 10^{-3} \text{ GeV}\}; \{m_{H^{\pm\pm}} > 200 \text{ GeV}\}. \quad (3.14)$$

The precision study of  $h_{\text{SM}}$  at the LHC restricts the large mixing of the doublet-like scalar with the triplet-like neutral scalar as the observed  $\sim 125$  GeV Higgs boson is more SM-like. Therefore, we limit our scan to tiny  $\theta_t$  values to allow minimum mixing and maintain the nature of the Higgs boson SM-like. However, loop-induced decays of the SM-like Higgs boson

---

<sup>1</sup>In this article, we focus on a similar region of parameter space of the type-II seesaw model that is considered in reference [31]. Note that, from the EW precision data  $\Delta m$  is upper bounded and it has to be below 40 GeV.

( $h_{\text{SM}}$ ), such as  $h_{\text{SM}} \rightarrow \gamma\gamma$ , can still deviate significantly from the experimentally observed limits of the signal strength of the same decay channel even at small  $\sin\theta_t$  value. The variation of the signal strength of the  $h_{\text{SM}} \rightarrow \gamma\gamma$  decay mode in the above-discussed region of parameter space in equation 3.14 is discussed in reference [31, 62]. Note that, at relatively small triplet-like charged Higgs bosons and larger portal couplings ( $\lambda_1, \lambda_4$ ), the decay width of the SM Higgs into a photon pair significantly deviates from the observed limits [63, 64].

In this article, we analyze the thermal history of the scalar potential and determine the region of the parameter space that features an FOEWPT in the early Universe. After such an FOEWPT, the broken phase eventually evolves to the EW minimum of the potential at  $T = 0$ . We use **CosmoTransitions** [37] to study the evolution of various minima with temperature as well as the transition between the various minima of the scalar potential at finite temperature. The theoretical details for the study of phase transition in the early Universe, such as the field-dependent mass relations of various degrees of freedom and the daisy coefficients (to estimate the thermal mass corrections) are described in detail in reference [31]. Furthermore, we analyse the dilution factor of the thermal relic density caused by such an FOEWPT. Various DM observables, such as its relic density, its freeze-out temperature and its spin-independent direct detection cross-section have been estimated using **micrOMEGAs** (v4.3) [65].

## 4 Result

With the description of the model and various experimental constraints in section 3, we move on to present our results. we discuss the feasibility of a scalar DM with a mass around/above 1 TeV in our scenario, as well as the range of the freeze-out temperatures for such heavy DM in subsection 4.1. Furthermore, in subsection 4.2, we estimate the dilution factor of the DM relic density due to an FOEWPT. We discuss the region of parameter space of this model where the dilution factor becomes significantly large. As pointed out in the introduction, we further study the dependencies of the dilution factor on the model parameters, the nucleation temperature and on the strength and the duration of the phase transition. Finally, in subsection 4.3, we discuss the connection between the production of stochastic GW and the dilution factor as a result of an FOEWPT.

### 4.1 TeV-scale scalar DM and the freeze-out temperature

The phenomenology of the scalar DM in our situation is discussed in this subsection. The DM annihilates in three ways to freeze out in the early Universe and those processes are given by: DM annihilation (a)  $S S^* \rightarrow \text{SM SM}$ , (b)  $S S^* \rightarrow X Y$ ;  $\{X, Y\} = \{H^0, A^0, H^\pm, H^{\pm\pm}\}$  and DM semi-annihilation (c)  $S S \rightarrow S U$ ;  $\{U\} = \{h_{\text{SM}}, H^0\}$ . The DM Higgs portal interactions  $\lambda_{SH}(S^*S)(H^\dagger H)$  and  $\lambda_{S\Delta}(S^*S)\text{Tr}[\Delta^\dagger \Delta]$  control the DM-annihilation processes (a) and (b), respectively, whereas the DM semi-annihilation processes are initiated via the cubic interaction term  $\mu_3(S^3 + S^{*3})$  in the scalar potential.<sup>2</sup> Therefore, the DM relic density

---

<sup>2</sup>Note that at small  $v_t$ -limit the DM semi-annihilation process  $S S \rightarrow S H^0$  and the  $S$ -channel neutral triplet-like scalar  $H^0$ -mediated DM-annihilation process are high suppressed.

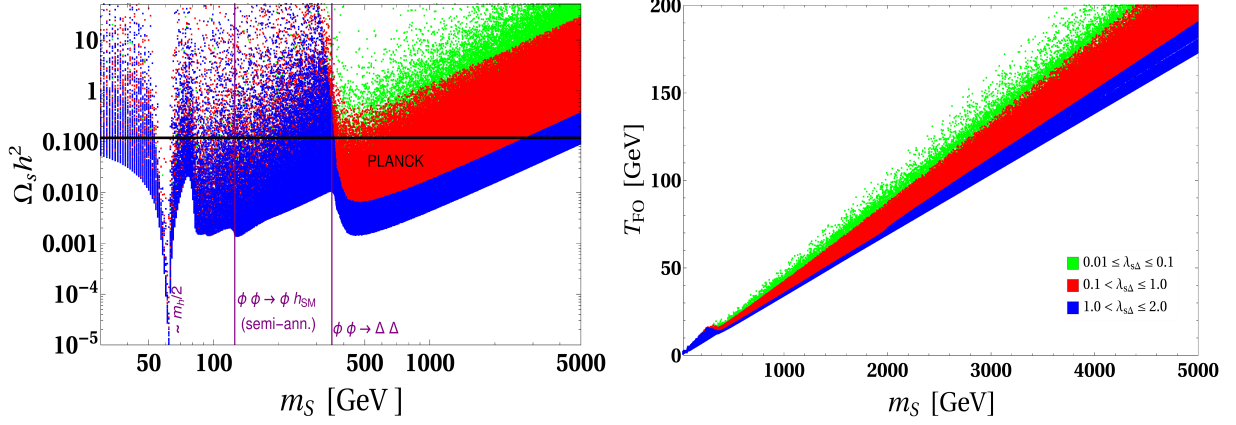


**Figure 1.** [Left plot:] Variation of relic density ( $\Omega_s h^2$ ) as a function of DM mass ( $m_s$ ) in GeV for different ranges  $\lambda_{S\Delta}$  :  $0.01 \leq \lambda_{S\Delta} \leq 0.1$  (green),  $0.1 < \lambda_{S\Delta} \leq 1.0$  (red),  $1.0 < \lambda_{S\Delta} \leq 2.0$  (blue) and  $0.001 < \lambda_{SH} \leq 0.5$ . [Right plot:] Variation of freeze-out temperature ( $T_{FO}$ ) with  $m_s$  for same range of  $\lambda_{S\Delta}$  and  $\lambda_{SH}$ . In these two plots  $\mu_3 = m_s$  and the triplet sector parameters are fixed at  $m_{H^0, A^0} = 367.7$  GeV,  $m_{H^\pm} = 387.5$  GeV,  $m_{H^{\pm\pm}} = 406.4$  GeV,  $\sin \theta_t = -1.03 \times 10^{-6}$ . In the left plot, on the vertical axis  $\Omega_s h^2$  is truncated at the value of 50 and on the horizontal axis  $m_s$  is considered up to 5 TeV. Black horizontal lines indicates the Planck observed DM relic density, i.e.,  $\Omega_{DM} h^2 = 0.120 \pm 0.001$ . The vertical black lines indicate opening of various DM annihilation channels. In the right plot, the horizontal axis is truncated at the value of  $T_{FO} = 200$  GeV.

varies as:

$$\Omega_S h^2 \propto \frac{1}{\langle \sigma v \rangle_{SS \rightarrow SM} + \langle \sigma v \rangle_{SS \rightarrow SU} + \langle \sigma v \rangle_{SS \rightarrow X} Y}. \quad (4.1)$$

In the left plot of figure 1, we illustrate the variation of  $\Omega_S h^2$  as a function of  $m_S$  while fixing the triplet-sector parameters at  $m_{H^0, A^0} = 367.7$  GeV,  $m_{H^\pm} = 387.5$  GeV,  $m_{H^{\pm\pm}} = 406.4$  GeV and  $\sin \theta_t = -1.03 \times 10^{-6}$  while the DM-Higgs interaction couplings are varied in the range of  $0.001 < \lambda_{SH} < 0.5$ ,  $0.01 < \lambda_{S\Delta} < 2$  and  $0 < m_s < 5$  TeV. Such a choice of parameters is considered to understand the dependencies of the phenomenology of DM on the model parameters. In the right plot of figure 1, we present the variation of the freeze-out temperature ( $T_{FO}$ ) with  $m_s$ . Different colours show different ranges of  $\lambda_{S\Delta}$  in these two plots. Colors in green, red and blue indicate  $0.01 \leq \lambda_{S\Delta} \leq 0.1$ ,  $0.1 < \lambda_{S\Delta} \leq 1.0$  and  $1.0 < \lambda_{S\Delta} \leq 2.0$ , respectively. The black dotted horizontal lines indicate the measured density of DM relics from the PLANCK experiment, i.e.,  $\Omega_{DM} h^2 = 0.120 \pm 0.001$  [1]. The equation 1 suggests that the relic density might rapidly decrease with growing DM mass as a result of the opening of new number-changing processes at a certain threshold DM mass. Such a phenomenon shows up in the left plot.

In the scenario where the DM mass is larger than the triplet-like scalar masses, the DM annihilation processes mentioned in the category ‘b’ open up and the four-point contact interaction term,  $\lambda_{S\Delta}(S^* S) \text{Tr}[\Delta^\dagger \Delta]$ , starts to contribute. A larger  $\lambda_{S\Delta}$  enhances the DM annihilation cross-sections and beyond a certain value, the DM annihilation cross-section

of the processes of the category ‘b’ becomes the dominant one compared with the other annihilation processes. Note that in the limit of small  $v_t$  and  $\sin \theta_t$ , the contribution of the  $H^0$ -mediated  $t$ -channel process to the DM direct detection spin-independent (DMDD-SI) cross-section is negligible. Therefore, the DMDD-SI cross-section mostly depends on  $\lambda_{SH}$  (mediated via  $h_{SM}$ ) and has an insignificant effect on the variation of  $\lambda_{S\Delta}$ . Thus, for a heavier DM, the region of parameter space with larger  $\lambda_{S\Delta}$  can meet the experimentally observed DM relic density criteria without increasing the DMDD-SI cross-section significantly. As a result, this model can accommodate a heavy ( $\sim$ TeV-scale) DM complying with various DM experimental constraints. The variation of  $T_{FO}$  with  $m_S$  in the right plot of figure 1 indicates that heavy  $m_S$  corresponds to larger  $T_{FO}$ . It follows roughly  $T_{FO} \sim m_S/25$  relation. The ratio  $m_S/T_{FO}$  changes with the variation of various portal couplings. It is worth noting that the DM mass has to be large ( $\gtrsim 1$  TeV) for the situation in which the DM freeze-out temperature is higher than the temperature at which the FOEWPT occurs in the scalar potential.

In order to obtain the DM abundance and the freeze-out temperature we first implement the model in `FeynRules` [66] and then the outputs are fed into `micrOMEGAs` [65]. Note that in the situation where an FOPT occurs around the electroweak scale in the scalar potential and the DM freeze-out temperature is larger than the phase transition temperature, the DM relic density and freeze-out temperature that are estimated using `micrOMEGAs` no longer remain valid. Such a scenario may appear for heavier DM ( $\gtrsim 1$  TeV). However, such a computation is outside the scope of this study, we preserve it for future work. The present work aims to quantify the dilution factor of the DM relic density caused by the FOEWPT due to the release of entropy, which is discussed in the next subsection.

## 4.2 Estimation of the dilution factor

In this subsection, we estimate the dilution factor of the DM relic density due to an FOPT along the  $h_d$ -field direction. In the region of parameter space we scan for this work, the triplet field values,  $h_t$ , at the various minima of the effective potential at finite temperature always remain tiny. The FOPT happens only along the  $h_d$ -field direction. Therefore, we only discuss the dilution factor due to this one-step FOPT. However, an FOPT can occur in the early Universe along the singlet-field direction, i.e., along the  $h_s$ -field direction. Such a phase transition demands a relatively low DM mass [31]. On the other hand, the dilution effect caused by the FOPT on the relic density becomes significant only when the DM mass is relatively large  $\gtrsim 1$  TeV. An FOPT along the  $h_s$ -field direction is unlikely to occur for such a heavy DM. Therefore, in the context of this work, the relevant FOPT is the transition that happens only along the  $h_d$ -field direction.

The variation of the dilution factor caused by an FOPT, calculated using equation 2.12, with the effective quartic coupling of the potential ( $\lambda_1 + \lambda_4$ ) has been shown in figure 2. The color in the palette indicates the mass of the doubly-charged Higgs. Note that the dilution factor increases with the increase of the effective quartic coupling  $\lambda_1 + \lambda_4$ . The color variation indicates that a decrease in  $m_{H^{\pm\pm}}$  enhances the dilution factor for a given value of  $\lambda_1 + \lambda_4$ . Thus, the parameter space with larger effective quartic couplings ( $\lambda_1, \lambda_4$ ) and lower  $m_{H^{\pm\pm}}$  are preferred for larger dilution factors resulting from an FOPT along the  $h_d$ -field direction.

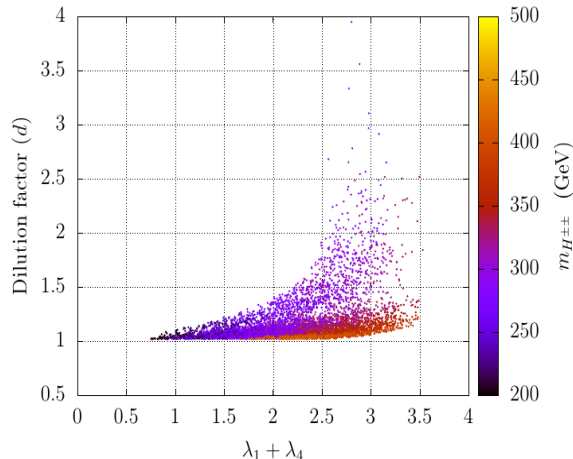


**Figure 2.** Variation of the dilution factor ( $d$ ) with the effective quartic coupling  $\lambda_1 + \lambda_4$ . The palette-color indicates  $m_{H^{\pm\pm}}$ .

One of the most critical parameters of the estimation of dilution is the temperature at which the FOPT occurs. Here, we discuss the correlations between the nucleation temperature ( $T_n$ ) of the phase transition and the dilution factor. Figure 3 represents the variation of the dilution factor with  $T_n$ . It indicates that the dilution factor increases with decreasing  $T_n$ . The palette color in the left plot indicates the difference between  $T_c$  and  $T_n$ , i.e.,  $\Delta T_{cn}$ . The variation in color indicates that the dilution factor also increases with an increasing  $\Delta T_{cn}$ . In the scenario with a small  $\Delta T_{cn}$ , the impact of dilution becomes insignificant due to negligible supercooling. As opposed to that, significant supercooling can occur for the large separations between  $T_c$  and  $T_n$ , which enhances the dilution factor. This result is consistent with the findings in references [25, 26, 67, 68]. The dependence of the supercooling with the dilution factor can be understood from the relation in equation 2.12. In the right plot of figure 3, the strength of the phase transition ( $\xi_n$ ) is defined as,  $\xi_n = \frac{\sqrt{\langle h_d(T_n) \rangle_{BP}^2 - \langle h_d(T_n) \rangle_{SP}^2}}{T_n}$  where ‘BP’ and ‘SP’ represent the broken phase and the symmetric phase, respectively.  $\xi_n$  is indicated by the palette color. The color variation indicates that the dilution factor increases with  $\xi_n$ . It is expected since a stronger FOPT often results in substantial supercooling, which enhances the dilution factor.

We find that the dilution factor can increase up to around 4 at  $T_n \sim 40$  GeV. On the other hand, the effect of dilution is almost negligible for  $T_n \gtrsim 120$  GeV. Therefore, the relic density would not be diluted if the DM freeze-out temperature,  $T_{FO}$ , is lower than 40 GeV. On the contrary, there would always be a considerable dilution of the relic density for any DM candidate that freezes out at temperatures larger than 120 GeV. As a result, the dilution effect would only be significant for significantly heavy DM.

The DMDD cross-section depends on the relic density of the DM in the present Universe. For the underabundant DM, the DMDD-SI cross-section scales with the factor  $f_{\text{scale}} = \frac{\Omega_{\text{DM}} h^2}{0.120}$ . The study of the dilution of relic density is crucial as it can rescue some of the samples which

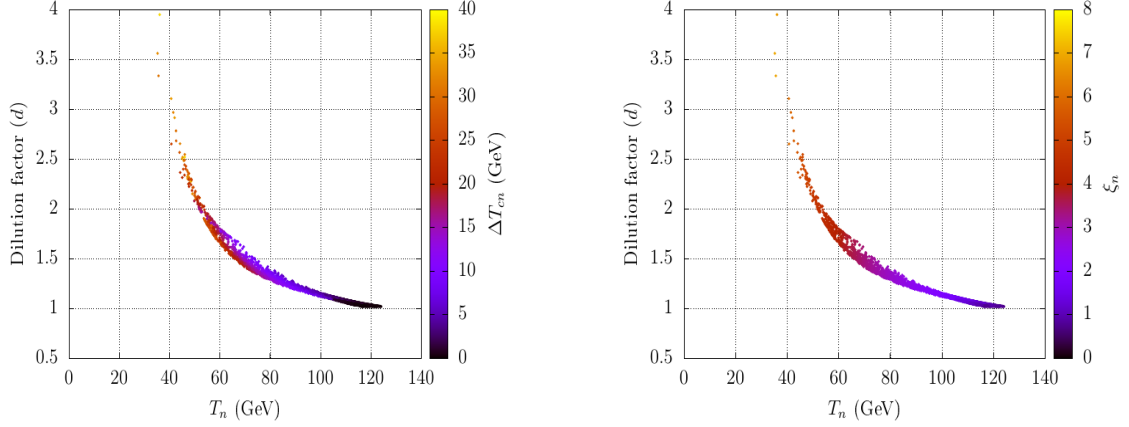


**Figure 3.** Variation of dilution factor ( $d$ ) with the nucleation temperature ( $T_n$ ) of the FOEWPT. The variation of the difference between the critical temperature and the nucleation temperature  $\Delta T_{cn}$  and the strength of the phase transition  $\xi_n$  are indicated via the palettes in the left and right plots, respectively.

are otherwise excluded from the DMDD experimental constraints from the various experiment such as XENON-1T [69] and PANDA-4T [70]. Additionally, such a dilution caused by FOPT can bring down the DM relic density value below the Planck experiment measured value and save the point that would otherwise be excluded due to the overabundance. Therefore, such an estimation of the dilution factor due to FOEWPT is crucial for the study of DM phenomenology. In addition, note that such an FOEWPT can generate a stochastic GW. Thus, in the following subsection, we shall discuss the connection between the dilution factor and the produced GW due to the FOEWPT.

### 4.3 Connection between the produced GW and the Dilution factor

Future proposed GW experiments might detect stochastic GW generated during an FOEWPT which also dilutes the relic density of DM. The dominant contribution of the GW peak intensity among the three mechanisms of the production of GW, as described in section 2, comes from the sound waves. The details of the estimation of GW intensity from the sound waves are presented in Appendix A. The GW peak amplitude can be found by putting  $f = f_{\text{SW}}$  in equation A.1. The peak frequency ( $f_{\text{SW}}$ ) is given in equation A.2.

In figure 4, we present the variation of the peak amplitudes with the peak frequencies of the produced GWs as a result of an FOEWPT. The dilution factor of the DM relic density caused by an FOEWPT is presented by the palette-color. Note that various future proposed space/ground-based GW experiments, such as LISA [17], ALIA [18], Taiji [19], TianQin [20], aLIGO+ [21], Big Bang Observer (BBO) [22] and Ultimate(U)-DECIGO [23], etc., have different regions of sensitivity over the peak intensity and the peak frequency range. Therefore, the study of the variation of the peak frequency and the peak amplitude of the produced GW is crucial for detecting the spectrum in future proposed GW experiments.



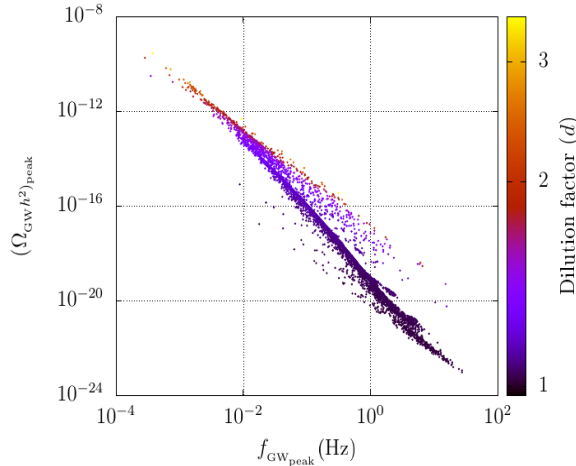


**Figure 4.** Variation of the GW peak amplitude  $(\Omega_{\text{GW}}h^2)_{\text{peak}}$  with the peak frequency  $(f_{\text{GW}_{\text{peak}}})$  estimated from the sound wave contribution. The palette-color shows the variation of the dilution factor  $(d)$ .

The color variation in figure 4 indicates that the dilution factor increases as both GW peak amplitude and peak frequency increase. Such a connection between GW intensity and dilution factor can be realised on their dependence on the strength of the phase transition,  $\xi_n$ . Thus, a stronger FOEWPT forecasts a bigger GW peak amplitude as well as a larger dilution factor. Therefore, observing the GW peak amplitude and the peak frequency in some of the future proposed GW experiments can reveal the range of the DM dilution factor of the DM relic density due to a release of entropy during the FOEWPT.

## 5 Conclusions

Despite many successes of the SM, it cannot explain the origin of the observed baryon asymmetry of the Universe, the non-vanishing masses of neutrinos and accommodate a DM candidate. In this article, we consider the  $Z_3$ -symmetric complex singlet scalar extended type-II seesaw model that can simultaneously provide solutions to these issues within a single framework. An SFOEWPT is one of the essential requirements for triggering EWBG that can generate the observed BAU at the electroweak scale. Such an FOEWPT could dilute the relic density of DM due to an injection of entropy and a release of latent heat.

In the current model, the triplet sector can modify the SM Higgs potential in favor of an FOEWPT along the  $h_d$ -field direction even when the singlet scalar fields are heavy. As a result, the singlet scalar DM can get heavier while still allowing for an FOEWPT in the scalar potential. In such a scenario, a significant dilution in the DM relic abundance is possible for a heavier DM that freezes out much before the FOEWPT takes place.

We find the regions of parameter space of the triplet sector of the scenario that corresponds to an FOEWPT and can generate a sizable amount of dilution. Such a region prefers



relatively light  $m_{H^{\pm\pm}}$  and larger effective quartic couplings  $\lambda_1 + \lambda_4$ . In the case of supercooling, the released entropy caused by the FOEWPT could dilute the DM relic density up to a factor of around 4 in our scenario. Furthermore, we show the variation of the dilution factor with the temperature at which the phase transition occurs. We note that the dilution factor increases with decreasing  $T_n$ . The difference between  $T_c$  and  $T_n$  is also an important factor in this estimation. A larger gap between  $T_c$  and  $T_n$  leads to a significant amount of supercooling during the phase transition which, in turn, enhances the dilution factor. DM relic density dilution starts only for  $T_n \lesssim 120$  GeV. Thus, the DM with a freeze-out temperature much larger than this, which is possible in this model, could experience significant dilution in its relic abundance. Such a dilution might retrieve some of the regions of parameter space that were previously ruled out by the measured value of the DM relic density and/or the latest constraints from the DM direct-detection experiments. On the contrary, there will be no dilution in the abundance of DM whose freeze-out temperature is  $\lesssim 40$  GeV and such a scenario corresponds to a relatively light DM ( $\lesssim 1$  TeV).

As is well known we also find that the dilution factor increases with the strength of the FOEWPT. Furthermore, in the early Universe, such an FOEWPT could have generated stochastic GW. Hence a connection between the dilution factor and the generation of the stochastic GW, as a result of an FOEWPT, is discussed. The dilution factor increases with GW peak amplitude and peak frequency. Therefore, observing peak amplitude and peak frequency of GW produced from an FOEWPT in some of the future proposed space/ground-based GW experiments can reveal the range of the DM dilution factor of the DM relic density due to the release of entropy during the same phase transition.

Dilution of the DM relic density is only possible in this model when the DM is heavy and an FOEWPT occurs in the early Universe. The type-II seesaw sector of this current model that can alter the SM-like Higgs potential in favor of an FOEWPT would get tested by studying the di-photon decays of the SM-like Higgs boson at the HL-LHC. A null-finding of new physics at the HL-LHC would rule out the possibility of an FOEWPT triggered by the triplet sector and hence the possibility of dilution of relic density of a TeV-scale DM in such a scenario.

## Acknowledgments

The work of SR is supported by the Department of Atomic Energy (DAE), Government of India for the Regional Centre for Accelerator-based Particle Physics (RECAPP) at Harish-Chandra Research Institute (HRI). SR is also supported by the excellence in research award from Infosys. SR would like to thank AseshKrishna Datta and Yang Zhang for useful discussions. SR also acknowledges the use of High-Performance Scientific cluster computing facilities at HRI and RECAPP.

## Appendix

### A Contribution of sound waves to gravitational waves power spectrum

The dominant contribution to the total GW power spectrum coming from the sound waves,  $\Omega_{\text{sw}} h^2$ , is given by [41–44]

$$\Omega_{\text{SW}} h^2 = 2.65 \times 10^{-6} \Upsilon(\tau_{\text{SW}}) \left( \frac{\beta}{H_*} \right)^{-1} v_w \left( \frac{\kappa_v \alpha}{1 + \alpha} \right)^2 \left( \frac{g_*}{100} \right)^{-\frac{1}{3}} \left( \frac{f}{f_{\text{SW}}} \right)^3 \left[ \frac{7}{4 + 3 \left( \frac{f}{f_{\text{SW}}} \right)^2} \right]^{\frac{7}{2}}, \quad (\text{A.1})$$

where  $f_{\text{SW}}$  is the present day peak frequency and is given by

$$f_{\text{SW}} = 1.9 \times 10^{-5} \text{ Hz} \left( \frac{1}{v_w} \right) \left( \frac{\beta}{H_*} \right) \left( \frac{T_n}{100 \text{ GeV}} \right) \left( \frac{g_*}{100} \right)^{\frac{1}{6}}. \quad (\text{A.2})$$

In the above relations,  $H_*$  is the Hubble rate just after the end of GW production and  $T_*$  is the temperature at that time. For this work, we consider  $T_* \approx T_n$ . The dimensionless quantity that is related to the energy budget of the phase transition,  $\alpha$ , is defined as [71]

$$\alpha = \frac{\rho_{\text{vac}}}{\rho_{\text{rad}}^*} = \frac{1}{\rho_{\text{rad}}^*} \left[ T \frac{\partial \Delta V(T)}{\partial T} - \Delta V(T) \right] \Big|_{T_*}. \quad (\text{A.3})$$

The parameter  $\beta$  that estimates the inverse time duration of the phase transition is given by

$$\beta = - \frac{dS_3}{dt} \Big|_{t_*} \simeq \frac{\dot{\Gamma}}{\Gamma} = H_* T_* \frac{d(S_3/T)}{dT} \Big|_{T_*}. \quad (\text{A.4})$$

The parameter  $\kappa_v$  estimates the fraction of latent heat energy transferred into the bulk motion of the fluid and is given by [71]

$$\kappa_v \simeq \left[ \frac{\alpha}{0.73 + 0.083 \sqrt{\alpha} + \alpha} \right]. \quad (\text{A.5})$$

The suppression factor  $\Upsilon(\tau_{\text{SW}})$  appears due to the finite lifetime of sound waves and is given by [72, 73]

$$\Upsilon(\tau_{\text{SW}}) = 1 - \frac{1}{\sqrt{1 + 2\tau_{\text{SW}} H_*}}, \quad (\text{A.6})$$

Where  $\tau_{\text{sw}}$  is the lifetime of the sound waves. It can be estimated from the time scale in which the turbulence develops. It is approximately given by [74, 75]:

$$\tau_{\text{sw}} \sim \frac{R_*}{\bar{U}_f}, \quad (\text{A.7})$$

where  $R_*$  denotes the mean bubble separation related to the phase transition duration. It is given by  $R_* = (8\pi)^{1/3} v_w / \beta$  [72, 76]. The quantity  $\bar{U}_f$  represents the root-mean-squared (RMS) velocity and it is given by  $\bar{U}_f = \sqrt{3\kappa_v \alpha / 4}$  [76, 77]. More details related to the computation of the GW power spectrum from the FOPT in the present model have been discussed in reference [31].

## References

- [1] N. Aghanim *et al.* [Planck], *Astron. Astrophys.* **641** (2020), A6 [erratum: *Astron. Astrophys.* **652** (2021), C4] doi:10.1051/0004-6361/201833910 [arXiv:1807.06209 [astro-ph.CO]].
- [2] G. Aad *et al.* [ATLAS], *Phys. Lett. B* **716** (2012), 1-29 doi:10.1016/j.physletb.2012.08.020 [arXiv:1207.7214 [hep-ex]].
- [3] S. Chatrchyan *et al.* [CMS], *Phys. Lett. B* **716** (2012), 30-61 doi:10.1016/j.physletb.2012.08.021 [arXiv:1207.7235 [hep-ex]].
- [4] D. A. Kirzhnits and A. D. Linde, *Phys. Lett. B* **42** (1972), 471-474 doi:10.1016/0370-2693(72)90109-8
- [5] K. Kajantie, M. Laine, K. Rummukainen and M. E. Shaposhnikov, *Nucl. Phys. B* **493** (1997), 413-438 doi:10.1016/S0550-3213(97)00164-8 [arXiv:hep-lat/9612006 [hep-lat]].
- [6] P. A. R. Ade *et al.* [Planck], *Astron. Astrophys.* **594** (2016), A13 doi:10.1051/0004-6361/201525830 [arXiv:1502.01589 [astro-ph.CO]].
- [7] A. D. Sakharov, *Pisma Zh. Eksp. Teor. Fiz.* **5** (1967), 32-35 doi:10.1070/PU1991v034n05ABEH002497
- [8] M. Trodden, *Rev. Mod. Phys.* **71** (1999), 1463-1500 doi:10.1103/RevModPhys.71.1463 [arXiv:hep-ph/9803479 [hep-ph]].
- [9] G. W. Anderson and L. J. Hall, *Phys. Rev. D* **45** (1992), 2685-2698 doi:10.1103/PhysRevD.45.2685
- [10] P. Huet and A. E. Nelson, *Phys. Rev. D* **53** (1996), 4578-4597 doi:10.1103/PhysRevD.53.4578 [arXiv:hep-ph/9506477 [hep-ph]].
- [11] D. E. Morrissey and M. J. Ramsey-Musolf, *New J. Phys.* **14** (2012), 125003 doi:10.1088/1367-2630/14/12/125003 [arXiv:1206.2942 [hep-ph]].
- [12] M. Quiros, [arXiv:hep-ph/9901312 [hep-ph]].
- [13] B. P. Abbott *et al.* [LIGO Scientific and Virgo], *Phys. Rev. Lett.* **116** (2016) no.6, 061102 doi:10.1103/PhysRevLett.116.061102 [arXiv:1602.03837 [gr-qc]].
- [14] B. P. Abbott *et al.* [LIGO Scientific and Virgo], *Phys. Rev. Lett.* **119** (2017) no.16, 161101 doi:10.1103/PhysRevLett.119.161101 [arXiv:1710.05832 [gr-qc]].
- [15] B. P. Abbott *et al.* [LIGO Scientific and Virgo], *Phys. Rev. X* **9** (2019) no.3, 031040 doi:10.1103/PhysRevX.9.031040 [arXiv:1811.12907 [astro-ph.HE]].
- [16] R. Abbott *et al.* [LIGO Scientific and Virgo], *Phys. Rev. X* **11** (2021), 021053 doi:10.1103/PhysRevX.11.021053 [arXiv:2010.14527 [gr-qc]].
- [17] P. Amaro-Seoane *et al.* [LISA], [arXiv:1702.00786 [astro-ph.IM]].
- [18] X. Gong, Y. K. Lau, S. Xu, P. Amaro-Seoane, S. Bai, X. Bian, Z. Cao, G. Chen, X. Chen and Y. Ding, *et al.* *J. Phys. Conf. Ser.* **610** (2015) no.1, 012011 doi:10.1088/1742-6596/610/1/012011 [arXiv:1410.7296 [gr-qc]].
- [19] W. R. Hu and Y. L. Wu, *Natl. Sci. Rev.* **4** (2017) no.5, 685-686 doi:10.1093/nsr/nwx116
- [20] J. Luo *et al.* [TianQin], *Class. Quant. Grav.* **33** (2016) no.3, 035010 doi:10.1088/0264-9381/33/3/035010 [arXiv:1512.02076 [astro-ph.IM]].

- [21] G. M. Harry [LIGO Scientific], *Class. Quant. Grav.* **27** (2010), 084006  
doi:10.1088/0264-9381/27/8/084006
- [22] V. Corbin and N. J. Cornish, *Class. Quant. Grav.* **23** (2006), 2435-2446  
doi:10.1088/0264-9381/23/7/014 [arXiv:gr-qc/0512039 [gr-qc]].
- [23] H. Kudoh, A. Taruya, T. Hiramatsu and Y. Himemoto, *Phys. Rev. D* **73** (2006), 064006  
doi:10.1103/PhysRevD.73.064006 [arXiv:gr-qc/0511145 [gr-qc]].
- [24] A. Megevand, *Phys. Rev. D* **69** (2004), 103521 doi:10.1103/PhysRevD.69.103521  
[arXiv:hep-ph/0312305 [hep-ph]].
- [25] A. Megevand and A. D. Sanchez, *Phys. Rev. D* **77** (2008), 063519  
doi:10.1103/PhysRevD.77.063519 [arXiv:0712.1031 [hep-ph]].
- [26] C. Wainwright and S. Profumo, *Phys. Rev. D* **80** (2009), 103517  
doi:10.1103/PhysRevD.80.103517 [arXiv:0909.1317 [hep-ph]].
- [27] D. Chung, A. Long and L. T. Wang, *Phys. Rev. D* **84** (2011), 043523  
doi:10.1103/PhysRevD.84.043523 [arXiv:1104.5034 [astro-ph.CO]].
- [28] Y. Xiao, J. M. Yang and Y. Zhang, [arXiv:2207.14519 [hep-ph]].
- [29] Y. Fukuda *et al.* [Super-Kamiokande], *Phys. Rev. Lett.* **81** (1998), 1562-1567  
doi:10.1103/PhysRevLett.81.1562 [arXiv:hep-ex/9807003 [hep-ex]].
- [30] Q. R. Ahmad *et al.* [SNO], *Phys. Rev. Lett.* **87** (2001), 071301  
doi:10.1103/PhysRevLett.87.071301 [arXiv:nucl-ex/0106015 [nucl-ex]].
- [31] P. Ghosh, T. Ghosh and S. Roy, [arXiv:2211.15640 [hep-ph]].
- [32] M. Aguilar *et al.* [AMS], *Phys. Rev. Lett.* **113** (2014), 121102  
doi:10.1103/PhysRevLett.113.121102
- [33] G. Ambrosi *et al.* [DAMPE], *Nature* **552** (2017), 63-66 doi:10.1038/nature24475  
[arXiv:1711.10981 [astro-ph.HE]].
- [34] S. Abdollahi *et al.* [Fermi-LAT], *Phys. Rev. D* **95** (2017) no.8, 082007  
doi:10.1103/PhysRevD.95.082007 [arXiv:1704.07195 [astro-ph.HE]].
- [35] X. Qi and H. Sun, [arXiv:2104.01045 [hep-ph]].
- [36] M. S. Turner, E. J. Weinberg and L. M. Widrow, *Phys. Rev. D* **46** (1992), 2384-2403  
doi:10.1103/PhysRevD.46.2384
- [37] C. L. Wainwright, *Comput. Phys. Commun.* **183** (2012), 2006-2013  
doi:10.1016/j.cpc.2012.04.004 [arXiv:1109.4189 [hep-ph]].
- [38] R. Apreda, M. Maggiore, A. Nicolis and A. Riotto, *Nucl. Phys. B* **631** (2002), 342-368  
doi:10.1016/S0550-3213(02)00264-X [arXiv:gr-qc/0107033 [gr-qc]].
- [39] A. Kosowsky, M. S. Turner and R. Watkins, *Phys. Rev. Lett.* **69** (1992), 2026-2029  
doi:10.1103/PhysRevLett.69.2026
- [40] A. Kosowsky, M. S. Turner and R. Watkins, *Phys. Rev. D* **45** (1992), 4514-4535  
doi:10.1103/PhysRevD.45.4514
- [41] M. Hindmarsh, S. J. Huber, K. Rummukainen and D. J. Weir, *Phys. Rev. Lett.* **112** (2014), 041301 doi:10.1103/PhysRevLett.112.041301 [arXiv:1304.2433 [hep-ph]].

- [42] J. T. Giblin, Jr. and J. B. Mertens, JHEP **12** (2013), 042 doi:10.1007/JHEP12(2013)042 [arXiv:1310.2948 [hep-th]].
- [43] J. T. Giblin and J. B. Mertens, Phys. Rev. D **90** (2014) no.2, 023532 doi:10.1103/PhysRevD.90.023532 [arXiv:1405.4005 [astro-ph.CO]].
- [44] M. Hindmarsh, S. J. Huber, K. Rummukainen and D. J. Weir, Phys. Rev. D **92** (2015) no.12, 123009 doi:10.1103/PhysRevD.92.123009 [arXiv:1504.03291 [astro-ph.CO]].
- [45] C. Caprini and R. Durrer, Phys. Rev. D **74** (2006), 063521 doi:10.1103/PhysRevD.74.063521 [arXiv:astro-ph/0603476 [astro-ph]].
- [46] T. Kahniashvili, A. Kosowsky, G. Gogoberidze and Y. Maravin, Phys. Rev. D **78** (2008), 043003 doi:10.1103/PhysRevD.78.043003 [arXiv:0806.0293 [astro-ph]].
- [47] T. Kahniashvili, L. Campanelli, G. Gogoberidze, Y. Maravin and B. Ratra, Phys. Rev. D **78** (2008), 123006 [erratum: Phys. Rev. D **79** (2009), 109901] doi:10.1103/PhysRevD.78.123006 [arXiv:0809.1899 [astro-ph]].
- [48] T. Kahniashvili, L. Kisslinger and T. Stevens, Phys. Rev. D **81** (2010), 023004 doi:10.1103/PhysRevD.81.023004 [arXiv:0905.0643 [astro-ph.CO]].
- [49] C. Caprini, R. Durrer and G. Servant, JCAP **12** (2009), 024 doi:10.1088/1475-7516/2009/12/024 [arXiv:0909.0622 [astro-ph.CO]].
- [50] L. Kisslinger and T. Kahniashvili, Phys. Rev. D **92** (2015) no.4, 043006 doi:10.1103/PhysRevD.92.043006 [arXiv:1505.03680 [astro-ph.CO]].
- [51] G. Aad *et al.* [ATLAS], Eur. Phys. J. C **72** (2012), 2244 doi:10.1140/epjc/s10052-012-2244-2 [arXiv:1210.5070 [hep-ex]].
- [52] S. Chatrchyan *et al.* [CMS], Eur. Phys. J. C **72** (2012), 2189 doi:10.1140/epjc/s10052-012-2189-5 [arXiv:1207.2666 [hep-ex]].
- [53] G. Aad *et al.* [ATLAS], JHEP **03** (2015), 041 doi:10.1007/JHEP03(2015)041 [arXiv:1412.0237 [hep-ex]].
- [54] V. Khachatryan *et al.* [CMS], Phys. Rev. Lett. **114** (2015) no.5, 051801 doi:10.1103/PhysRevLett.114.051801 [arXiv:1410.6315 [hep-ex]].
- [55] [CMS], CMS-PAS-HIG-14-039.
- [56] [CMS], CMS-PAS-HIG-16-036.
- [57] M. Aaboud *et al.* [ATLAS], Eur. Phys. J. C **78** (2018) no.3, 199 doi:10.1140/epjc/s10052-018-5661-z [arXiv:1710.09748 [hep-ex]].
- [58] A. M. Sirunyan *et al.* [CMS], Phys. Rev. Lett. **120** (2018) no.8, 081801 doi:10.1103/PhysRevLett.120.081801 [arXiv:1709.05822 [hep-ex]].
- [59] M. Aaboud *et al.* [ATLAS], Eur. Phys. J. C **79** (2019) no.1, 58 doi:10.1140/epjc/s10052-018-6500-y [arXiv:1808.01899 [hep-ex]].
- [60] G. Aad *et al.* [ATLAS], JHEP **06** (2021), 146 doi:10.1007/JHEP06(2021)146 [arXiv:2101.11961 [hep-ex]].
- [61] S. Ashanujjaman and K. Ghosh, JHEP **03** (2022), 195 doi:10.1007/JHEP03(2022)195 [arXiv:2108.10952 [hep-ph]].

- [62] R. Zhou, L. Bian and Y. Du, JHEP **08** (2022), 205 doi:10.1007/JHEP08(2022)205 [arXiv:2203.01561 [hep-ph]].
- [63] [ATLAS], [arXiv:2207.00348 [hep-ex]].
- [64] A. M. Sirunyan *et al.* [CMS], JHEP **07** (2021), 027 doi:10.1007/JHEP07(2021)027 [arXiv:2103.06956 [hep-ex]].
- [65] G. Belanger, F. Boudjema, A. Pukhov and A. Semenov, Comput. Phys. Commun. **176** (2007), 367-382 doi:10.1016/j.cpc.2006.11.008 [arXiv:hep-ph/0607059 [hep-ph]].
- [66] A. Alloul, N. D. Christensen, C. Degrande, C. Duhr and B. Fuks, Comput. Phys. Commun. **185** (2014), 2250-2300 doi:10.1016/j.cpc.2014.04.012 [arXiv:1310.1921 [hep-ph]].
- [67] L. Bian and Y. L. Tang, JHEP **12** (2018), 006 doi:10.1007/JHEP12(2018)006 [arXiv:1810.03172 [hep-ph]].
- [68] L. Bian and X. Liu, Phys. Rev. D **99** (2019) no.5, 055003 doi:10.1103/PhysRevD.99.055003 [arXiv:1811.03279 [hep-ph]].
- [69] E. Aprile *et al.* [XENON], Phys. Rev. Lett. **121** (2018) no.11, 111302 doi:10.1103/PhysRevLett.121.111302 [arXiv:1805.12562 [astro-ph.CO]].
- [70] Y. Meng *et al.* [PandaX-4T], Phys. Rev. Lett. **127** (2021) no.26, 261802 doi:10.1103/PhysRevLett.127.261802 [arXiv:2107.13438 [hep-ex]].
- [71] J. R. Espinosa, T. Konstandin, J. M. No and G. Servant, JCAP **06** (2010), 028 doi:10.1088/1475-7516/2010/06/028 [arXiv:1004.4187 [hep-ph]].
- [72] H. K. Guo, K. Sinha, D. Vagie and G. White, JCAP **01** (2021), 001 doi:10.1088/1475-7516/2021/01/001 [arXiv:2007.08537 [hep-ph]].
- [73] M. B. Hindmarsh, M. Lüben, J. Lumma and M. Pauly, SciPost Phys. Lect. Notes **24** (2021), 1 doi:10.21468/SciPostPhysLectNotes.24 [arXiv:2008.09136 [astro-ph.CO]].
- [74] U. L. Pen and N. Turok, Phys. Rev. Lett. **117** (2016) no.13, 131301 doi:10.1103/PhysRevLett.117.131301 [arXiv:1510.02985 [astro-ph.CO]].
- [75] M. Hindmarsh, S. J. Huber, K. Rummukainen and D. J. Weir, Phys. Rev. D **96** (2017) no.10, 103520 [erratum: Phys. Rev. D **101** (2020) no.8, 089902] doi:10.1103/PhysRevD.96.103520 [arXiv:1704.05871 [astro-ph.CO]].
- [76] M. Hindmarsh and M. Hijazi, JCAP **12** (2019), 062 doi:10.1088/1475-7516/2019/12/062 [arXiv:1909.10040 [astro-ph.CO]].
- [77] D. J. Weir, Phil. Trans. Roy. Soc. Lond. A **376** (2018) no.2114, 20170126 doi:10.1098/rsta.2017.0126 [arXiv:1705.01783 [hep-ph]].